Journal of Environmental Management 321 (2022) 115927

Contents lists available at ScienceDirect

Journal of Environmental Management

journal homepage: www.elsevier.com/locate/jenvman

Research article

Pathways and efficiency of nitrogen attenuation in wastewater effluent through soil aquifer treatment

Alex Abu [a,b,*], Raúl Carrey [a,b], Cristina Valhondo [c,d,e], Cristina Domènech [a,b], Albert Soler [a,b], Lurdes Martínez-Landa [f,g], Silvia Diaz-Cruz [e], Jesús Carrera [e,g], Neus Otero [a,b,h]

[a] Grup MAiMA, SGR Mineralogia Aplicada, Geoquímica I Geomicrobiologia, Departament de Mineralogia, Petrologia I Geologia Aplicada, Facultat de Ciències de La Terra, Universitat de Barcelona (UB), 08028, Barcelona, Catalonia, Spain
[b] Institut de Recerca de L'Aigua (IdRA), Universitat de Barcelona (UB), 08001, Barcelona, Catalonia, Spain
[c] Université de Montpellier. UMR 5243 Géosciences Montpellier. 300 Avenue Emile Jeanbrau CC MSE. 34095, Montpellier, France
[d] Université de Montpellier. UMR 5569 HydroSciences Montpellier. 15 Avenue Charles Flahault-BP 14491. 34093, Montpellier. France
[e] Institute of Environmental Assessment and Water Research (IDAEA). Severo Ochoa Excellence Center. Spanish National Research Council (CSIC), Jordi Girona 18-24, 08034 Barcelona, Spain
[f] Department of Civil and Environmental Engineering, Universitat Politecnica de Catalunya (UPC), Jordi Girona 1-3, 08034 Barcelona, Spain
[g] Hydrogeology Group (UPC-CSIC), Associate Unit, Jordi Girona, 08034 Barcelona, Spain
[h] Serra Húnter Fellowship. Generalitat de Catalunya, Catalonia, Spain

ARTICLE INFO

Keywords:
Isotopic fractionation
Enhanced biological denitrification
Permeable reactive barrier
Soil aquifer treatment
Nitrification
Denitrification

ABSTRACT

Soil Aquifer Treatment (SAT) is used to increase groundwater resources and enhance the water quality of wastewater treatment plant (WWTP) effluents. The resulting water quality needs to be assessed. In this study, we investigate attenuation pathways of nitrogen (N) compounds (predominantly NH_4^+) from a secondary treatment effluent in pilot SAT systems: both a conventional one (SAT-Control system) and one operating with a permeable reactive barrier (PRB) to provide extra dissolved organic carbon to the recharged water. The goal is to evaluate the effectiveness of the two systems regarding N compounds by means of chemical and isotopic tools. Water chemistry (NO_3^-, NH_4^+, Non-Purgeable Dissolved Organic Carbon (NPDOC), and O_2) and isotopic composition of NO_3^- ($\delta^{15}N$–NO_3^- and $\delta^{18}O$–NO_3^-) and NH_4^+ ($\delta^{15}N$–NH_4^+) were monitored in the inflow and at three different sections and depths along the aquifer flow path. Chemical and isotopic results suggest that coupled nitrification-denitrification were the principal mechanisms responsible for the migration and distribution of inorganic N in the systems and that nitrification rate decreased with depth. At the end of the study period, 66% of the total N in the solution was removed in the SAT-PRB system and 69% in the SAT-Control system, measured at the outlet of the systems. The residual N in solution in the SAT-PRB system had an approximately equal proportion of N–NH_4^+ and N–NO_3^- while in the SAT-Control system, the residual N in solution was primarily N–NO_3^-. Isotopic data also confirmed complete NO_3^- degradation in the systems from July to September with the possibility of mixing newly generated NO_3^- with the residual NO_3^- in the substrate pool.

1. Introduction

Nitrogen (N) pollution has become an important threat to water resources (Ren et al., 2014; Shi et al., 2019). Anthropogenic activities involving intensive fertilizer application and animal waste disposal represent the main global sources of N contamination (Arauzo, 2017; Zirkle et al., 2016). Furthermore, domestic, and industrial wastewater and septic-system effluents also serve as a significant source of N and contaminants of emerging concern (CECs). In manure and wastewater, N is mainly found as ammonium (NH_4^+) which, under aerobic conditions, is oxidized to nitrate (NO_3^-) (nitrification) as

$$NH_4^+ + 2O_2 \rightarrow NO_3^- + 2H^+ + H_2O \quad (1)$$

Nitrate contamination impairs its quality (Bourke et al., 2019). This fact has gained global attention in recent years as NO_3^- concentrations have been broadly reported above the 50 mgNO_3^-/L drinking water

* Corresponding author. Faculty of Earth Sciences, Department of Mineralogy, Petrology and Applied Geology, University of Barcelona, Martí i Franquès, s/n, 08028, Barcelona, Spain.
E-mail address: secretaria.ciencies.terra@ub.edu (A. Abu).

https://doi.org/10.1016/j.jenvman.2022.115927
Received 12 May 2022; Received in revised form 19 July 2022; Accepted 31 July 2022
Available online 19 August 2022

threshold value (European Union, 2006; 1991). The ingestion of NO_3^- contaminated water is linked to health hazards such as methemoglobinemia in infants and young children (WHO, 2004) and stomach cancer (Volkmer et al., 2005). Furthermore, nitrate is usually the limiting factor for algal growth, so increasing its concentration leads to eutrophication of groundwater dependent water bodies (Withers et al., 2014).

The main natural process to remove NO_3^- in aquifers is the reduction of NO_3^- to dinitrogen gas ($N_{2(g)}$) through a sequence of microbial reduction reactions (denitrification) (Korom, 1992; Matchett et al., 2019) (Fig. 1).

$$NO_3^- + 12H^+ + 10e^- \rightarrow N_2 + 6H_2O \quad (2)$$

Natural attenuation of NO_3^- can occur in anaerobic conditions in groundwater with oxygen levels below 1–2 mg/L (Singleton et al., 2007). Denitrifying bacteria responsible for these transformations are ubiquitous in surface and subsurface waters (Beauchamp et al., 1989) and they are predominantly facultative anaerobic denitrifying heterotrophs generating energy for growth and cell synthesis via the oxidation of organic compounds

$$CH_2O + 2NO_3^- + 7H^+ + 6e^- \rightarrow N_2 + HCO_3^- + 4H_2O \quad (3)$$

Autotrophic denitrifiers in groundwater use reduced inorganic compounds such as pyrite, sulfide, sulfite, S^0, HS^-, Fe(II), Mn(II) and H_2 as electron donors. Nonetheless, numerous studies have shown that the availability of electron donors is the main limiting factor for denitrification under natural aquifer conditions (King et al., 2012; Pabich et al., 2001). Other nitrogen attenuation pathways include (1) ammonium (NH_4^+) oxidation to nitrogen gas ($N_{2(g)}$) using nitrite (NO_2^-) as the electron acceptor in anaerobic conditions (anaerobic ammonium oxidation, or Anammox)) (2) anaerobic respiration by microorganisms using nitrate as electron acceptor (dissimilatory nitrate reduction to ammonium (DNRA)) and (3) plant uptake (assimilation). The main reactions involving the N transformation pathways are summarized in Fig. 1.

Microbial-mediated reactions tend to alter the distribution of the isotopes between the substrate and product pools. For this reason, stable isotopes of N in compounds such as NO_3^- and NH_4^+ ($\delta^{15}N$–NO_3^-, $\delta^{18}O$–NO_3^- and $\delta^{15}N$–NH_4^+) have been successfully used to study and characterize natural and induced denitrification processes (Adebowale et al., 2019; Carrey et al., 2013; Margalef-Marti et al., 2019) as well as nitrification processes (Castellano-Hinojosa et al., 2020).

Biologically enhanced denitrification (BED), which involves the biological stimulation of heterotrophic denitrification, has become a strategy to create optimized conditions by providing an external electron donor source in the aquifer (Critchley et al., 2014; Gibert et al., 2019; Margalef-Marti et al., 2019). This technology has evolved over the past decade in an attempt to clean up NO_3^- in groundwater to regulatory limits at a low cost. BED has been evaluated in several contexts and approaches like ex-situ groundwater remediation techniques (Baú and Mayer, 2008) and in situ bioremediation techniques such as in (I) artificial recharge ponds (Grau-Martínez et al., 2018), (II) permeable reactive barriers (PRB), reactive media installed perpendicular to flow path (Gibert et al., 2019; Valhondo et al., 2014) and (III) carbon injection systems (Critchley et al., 2014; Margalef-Marti et al., 2019).

Soil Aquifer Treatment (SAT) is a technique often employed to augment groundwater resources and improve water quality in water-stressed zones by promoting the infiltration of effluents from wastewater treatment plants (WWTPs) (Drewes, 2009; Maeng et al., 2010). Conventional wastewater treatment removes a large fraction of the biochemical oxygen demand and suspended solids from wastewater (Jokela et al., 2017; Naidoo and Olaniran, 2013) but is deficient in other water quality indicators such as N and organic compounds, such as CECs (Sonune and Ghate, 2004; Valhondo et al., 2014). N species and CECs are frequent in WWTP effluents (Díaz-Cruz and Barceló, 2008; Kuster et al., 2010; Maeng et al., 2010). The implementation of a PRB based on organic substrates at the bottom of infiltration basins has proven to increase the removal of NO_3^- and CECs from the recharged water SAT-PRB system using plant-based compost as reactive barriers has proven to successfully promote BED in artificial recharge ponds (Grau-Martínez et al., 2018). The barrier operates by releasing dissolved organic carbon, which acts as the electron donor to stimulate the consumption of diverse electron acceptors, including NO_3^- and favouring the CECs' biotransformation, improving the recharged water quality, and reducing NO_3^- leakage to the aquifer (Valhondo et al., 2015). The nitrogen cycle and the attenuation of organic contaminants across PRBs must be evaluated during the application SAT-PRB to assess its effectiveness. The rate of denitrification in SAT systems applying PRBs has shown to vary over time and is a function of the NO_3^- concentration reaching the reactive media, the residence time of NO_3^- within the reactive media and temperature (Robertson et al., 2008). Furthermore, wastewater often contains N as NH_4^+ rather than NO_3^-, affecting the efficiency of the SAT-PRB.

This work evaluates two pilot SAT systems that receive secondary treatment effluent from a WWTP located in the North of Catalonia, Spain. One system has a PRB consisting of plant compost blended with sand and a small fraction of clay (SAT-PRB system, T4) and the other has no PRB (SAT-Control system, T2) Fig. 2. The biochemical processes controlling the migration and speciation of the N compounds in the wastewater effluent are investigated to:

(1) understand the nitrogen cycle during SAT operations, so as to
(2) understand the prevailing processes affecting N in SAT, and to
(3) evaluate the potential of SAT and SAT-PRB to remove N

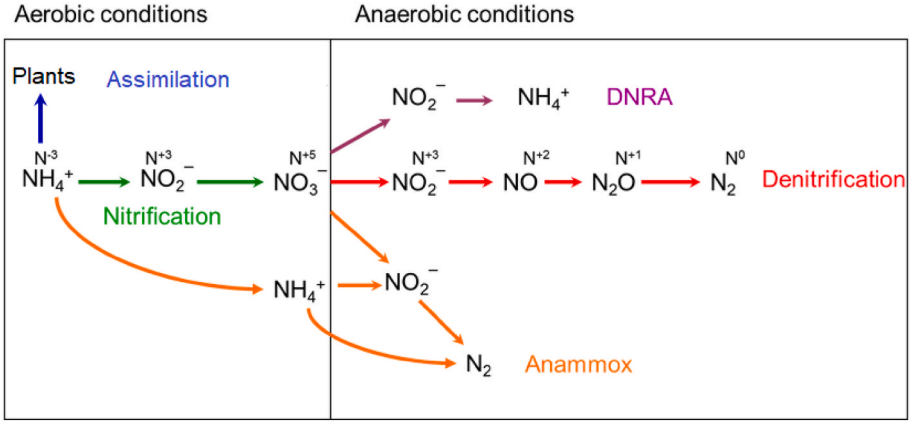

Fig. 1. Biogeochemical processes controlling the fate of N compounds in groundwater. Each coloured arrow indicates a specific N transformation pathway.

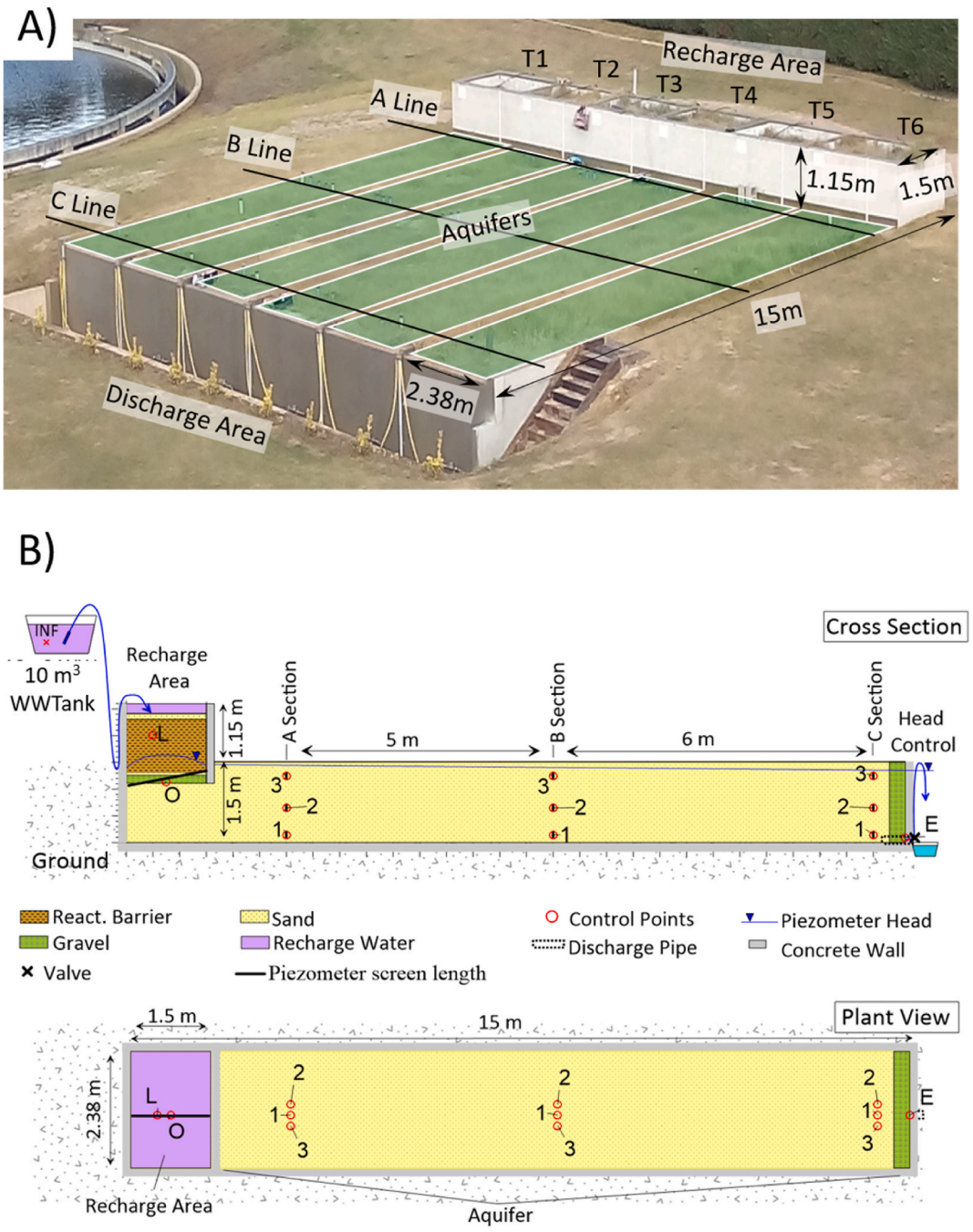

Fig. 2. A) General view of the experimental site, including recharge and discharge areas, piezometer sections and replicates T1 to T6; B) Cross-section and plan view of each system and monitoring points: O, A, B and C are the sampling sections along the flow path, INF = inflow water and E = outflow water; 1, 2 and 3 are the three sampling piezometers at each section (Deep, Middle and Shallow, respectively). A detailed description can be found in (Valhondo et al., 2020a,b).

2. Materials and methods

2.1. Site description

Six mesoscale SAT systems, named from T1 to T6, were built in the facility of a WWTP (Fig. 2A and B). Each system consists of a 15 × 2.38 × 1.5 m (length × width × height) sand canal, emulating the aquifer, coupled to a 1.5 × 2.38 × 1.15 m box emulating the infiltration basin. The infiltration box was filled with fine sand (ø = 0.1–0.2 mm) in the SAT-Control system (T2) and with a 1 m thick PRB in the remaining tanks. Plants were left to grow naturally at the surface of the infiltration areas and sand canals. Different plants, primarily grama grass, grew immediately after construction. The bottom 40 cm of each system was filled with coarse sand to favour the vertical flow to the discharge pipe (Fig. 2B). The systems were fed, during recharge episodes, with the effluent of the secondary treatment of the WWTP using PRIUS dosing pumps (EMEC, Rieti, Italy). The elevation of the discharge pipe, which collected the water from the bottom of the system, controlled the head in the outlet.

Ten piezometers were installed in each system for sampling and monitoring three distances from the infiltration area and at three depths. Piezometer "O" is a completely screened crosswise piezometer located just below the infiltration basin (Fig. 2B). Three 10-cm screened piezometers (1 at 1.3–1.4 m, 2 at 0.8–0.9 m, and 3 at 0.3–0.4 m depth) were placed in three sections (A, B, and C, at 1.5, 6.5, and 12.5 m from the recharge area, respectively) (Fig. 2B). Additionally, the inlet and outlet

of each system were sampled and monitored frequently. A detailed description of the systems can be found in (Valhondo et al., 2020b).

2.2. System performance and sampling collection

Four recharge episodes were performed during 2018. The first one lasted 27 days (from January, 5th through February, 1st) and aimed at conditioning the systems. The second, third and fourth recharge episodes (RE-2, RE-3 and RE-4) lasting 126 days (February to June), 65 days (July to September), and 74 days (October to January 2019), respectively, aimed at studying the performance of the systems.

An average flow rate of 0.4 m/d fed each system in all four recharge episodes. During these episodes, water samples were collected from the inlet, the monitoring points and the outlets of the systems for chemical and isotopic analyses. Field parameters (O_2, pH, Eh, Electrical Conductivity, and temperature) were measured during sampling using a multiparameter probe (YSI, Yellow Spring, OH, USA).

2.3. Analytical methods

Samples for Non-Purgeable Dissolved Organic Carbon (NPDOC) and chemical analyses were collected in muffled glass bottles, filtered through 0.22 μm membrane filters, acidified with HCl (for NPDOC analysis) or HNO_3 (for cations determination) and stored at 4 °C. NPDOC was measured with a TOC-VCSH analyser Shimadzu (Kyoto, Japan). Cations were analysed by inductively coupled plasma optical emission spectroscopy (ICP-OES) using an iCAP 6500 instrument (Thermo Fisher Scientific, Massachusetts, USA). NH_4^+ was analysed using an ORION Ion-Selective Electrode (ISE, Thermo Fisher Scientific, Massachusetts, USA). The main anions were measured by ion chromatography (IC) using a Dionex AQUION (Dionex, Sunnyvale, CA, USA) with an Ionpack AS9 2 × 250 mm column and Na_2CO_3 9 mM solution as eluent. Samples for NH_4^+, $\delta^{15}N–NH_4^+$, $\delta^{15}N–NO_3^-$, and $\delta^{18}O–NO_3^-$ analysis were kept frozen until analysed.

2.4. Isotopic methods

The nitrogen and oxygen isotopic abundance in nitrate ($\delta^{15}N–NO_3^-$ and $\delta^{18}O–NO_3^-$) were analysed using the cadmium (Cd) and sodium azide (NaN_3) reduction methods (McIlvin and Altabet, 2005; Ryabenko et al., 2009). The nitrogen isotopic abundance of NH_4^+ ($\delta^{15}N–NH_4^+$) was measured using the sodium hypobromite (NaBrO) and sodium azide reduction methods (Ryabenko et al., 2009; Zhang et al., 2007).

The standards used were the Vienna Standard Mean Oceanic Water (V-SMOW) for $\delta^{18}O–NO_3^-$ and $\delta^{18}O–NO_2^-$ analyses and AIR (Atmospheric N_2) for $\delta^{15}N–NO_3^-$ analyses. To correct the $\delta^{15}N–NO_3^-$ and $\delta^{18}O–NO_3^-$ values, three international standards (USGS 32, 34 and 35) and one internal laboratory standard (CCIT-IWS-NO3) were used. To correct $\delta^{15}N–NH_4^+$, two international standards (USGS-25 and IAEA-N2) and two internal laboratory standards (CCIT-IWS-NO2 and CCIT-IWS-NH4) were employed (Table 1). The samples for chemical and isotopic analyses were prepared at the laboratory of the MAiMA-UB research group and analysed at the Centres Científics i Tecnològics of the Universitat de Barcelona (CCiT-UB).

Table 1
Standards and reproducibility for isotopic analysis. International and laboratory (CCiT) standards used for the normalization of the results.

Analysis	Standard	Reference value [‰]	Reproducibility (1σ)
$\delta^{15}N–NO_3^-$	USGS-32,	+180.0	±1.0‰
	USGS-34,	−1.8	
	USGS-35	+2.7	
	CCiT-IWS	+16.9	
$\delta^{18}O–NO_3^-$	USGS-32,	+25.3	±1.5‰
	USGS-34,	−27.9	
	USGS-35	+57.3	
	CCiT-IWS	+28.5	
$\delta^{15}N–NH_4^+$	USGS-25	−30.4	±1.0‰
	IAEA-N2	+20.3	
	CCIT-IWS-NO2	−28.5	
	CCIT-IWS-NH4	−0.8	

3. Results

Results of NH_4^+, NO_3^-, NPDOC and O_2 concentration and isotopic data are available as Supplementary information (Table S1).

3.1. Chemical and isotopic results of inflow water

The average NH_4^+ concentration of the inflow water during RE-2, RE-3 and RE-4 varied significantly ranging from 0.93 to 5.54 mM. The measured NH_4^+ in the inflow water was higher during RE-3 (average of 4.2 mM, SD = 0.7, n = 20) while RE-2 and RE-4 measured similar NH_4^+ concentrations (Fig. 3). NO_3^- in the wastewater was below the detection limit (<0.01 mM) during all recharge episodes. The average O_2 measured was 0.27 mM (SD = 0.14, n = 18), 0.12 mM (SD = 0.09, n = 7) and 0.20 mM (SD = 0.03, n = 2) during RE-2, RE-3 and RE-4 respectively. RE-2 measured maximum and minimum NPDOC concentrations of 2.11 mM and 1.08 mM, respectively with an average of 1.41 mM and RE-3 measured maximum and minimum concentrations of 1.48 mM and 1.10 mM, respectively with an average concentration of 1.31 mM and RE-4 measured an average NPDOC concentration of 0.94 mM.

The $\delta^{15}N–NH_4^+$ of the inflow water showed considerable constant values with an average of +9.6‰ (n = 8 and SD = 0.80).

3.2. Chemical and isotopic results along the flow path of the systems

The average concentration of NH_4^+, NO_3^-, NPDOC and O_2 measured at the sampling points are shown in Fig. 3. RE-2 and RE-4 had similar NH_4^+ concentrations whereas slightly higher values were observed in RE-3 (Fig. 3) in both systems. For the 3 recharge episodes studied in both systems, NH_4^+ concentration progressively decreased from O to C and slightly increased from C to the outlet (E) for all recharge episodes. RE-2 showed a slight increase of NH_4^+ from O to A (Fig. 3). The NO_3^- concentrations displayed similar behaviour in both systems; measured NO_3^- concentrations were very low at O, A and B and significantly increased from C to the outlet (E) during all the recharge episodes (Fig. 3). NPDOC concentration showed, overall, a decrease from the inflow water, which showed no significant differences between recharge episodes, to the outlet (Fig. 3). The NPDOC concentration in the SAT-PRB increases at O compared to the inflow due to the DOC release from the RB, especially during RE-2 (2.065 ± 0.12 mM) and RE-3 (1.965 ± 0.46 mM) (Fig. 3). NPDOC concentration in the SAT-PRB system decreased progressively from O to E due to the oxidation of DOC. The concentration of O_2 decreased from the inlet (INF) to O in both systems during the three recharge episodes (Fig. 3). The O_2 concentration remained practically the same from the O to C and showed a slight increase from C to E except in RE-4 in both systems (Fig. 3).

3.3. Chemical and isotopic results with depth in the systems

Detailed profiles of NH_4^+, NO_3^-, NPDOC and O_2 with depth at 1, 2 and 3 points of A, B and C sections are presented in the supporting information (Table S2) and summarized in Fig. 4, where boxplots represent samples belonging to all the different depths at each section for each recharge episode. The concentration of NH_4^+ displayed an increasing profile with depth in monitoring points of section C of both systems and section A of the SAT-Control system, with an increase and a slight decrease in section B of both systems. NH_4^+ in the SAT-PRB system at section A which was high at the top showed decreasing and an increasing profile with depth (Fig. 4A). NO_3^- concentration showed no important change with depth at all sections in both systems (Fig. 4B). The NPDOC decreased from the top to the bottom at all sections of the

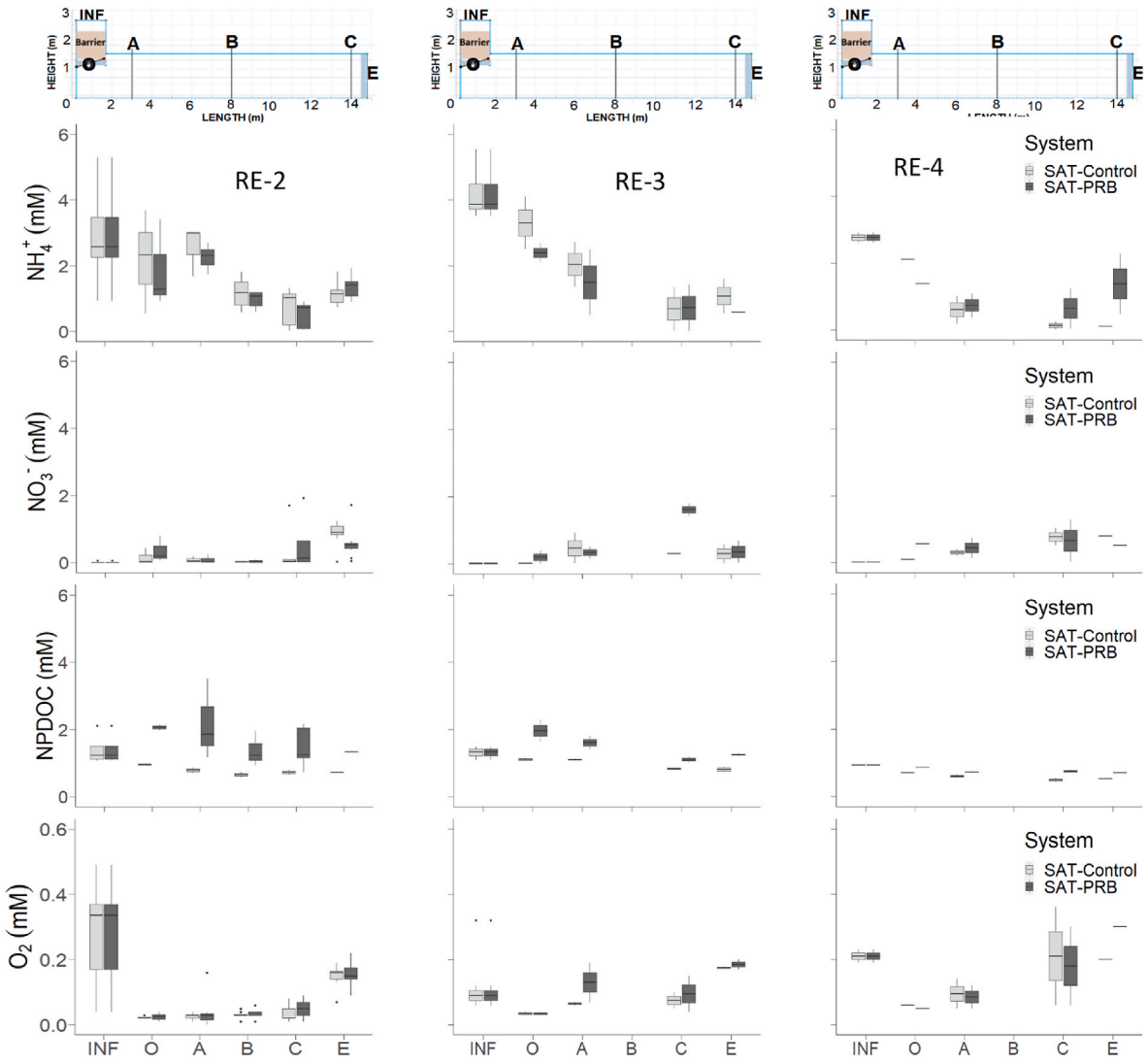

Fig. 3. Boxplots of NH_4^+, NPDOC, O_2 and NO_3^- aqueous concentration for all recharge episodes along the flow path. A scheme showing sections along the systems is also provided. Concentrations are indicated by the box plots and the outliers are represented by dots. Values in A, B, and C were calculated with the samples of the different depths at each section. INF = inflow water concentration and E is the outflow water concentration. First boxplot at each section (light grey) = SAT-Control system and the second boxplot (dark grey) = SAT-PRB system.

SAT-PRB system while exhibiting no significant decrease at all the sections of the SAT-Control system. The NPDOC in SAT-PRB systems was significantly higher due to the release of DOC from the RB (Fig. 4C). O_2 also slightly decreased from the top to the bottom of the systems at all the sampling points (Fig. 4D). The isotopic composition of NH_4^+ ($\delta^{15}N$–NH_4^+) in the SAT-Control system ranged from +8.4‰ to +29.4‰ where the lowest values were found in sample points O (just below the PRB) and the highest values were observed in sample points B and slight decrease afterwards at C and the outlet (Table S1). $\delta^{15}N$–NO_3^- and $\delta^{18}O$–NO_3^- ranged from +4.6‰ to +27‰ and from +9.2‰ to +41.9‰, respectively, where the highest values were observed in sample point O and decreased along the flow path with the lowest values observed in the outlet (Table S1). The isotopic composition of $\delta^{15}N$–NH_4^+ in the SAT-PRB system ranged from +9.6‰ to +34.7‰ where lower values were found in sample points O and increased along the flow path with the highest values observed in sample points C and slightly decreased at the outlet (Table S1). $\delta^{15}N$–NO_3^- and $\delta^{18}O$–NO_3^- ranged from +5.6‰ to +22.9‰ and from +10.5‰ to +38.2‰, respectively, where the highest values were observed in sample points A and decreased along the flow path with the lowest values observed in the outlet (Table S1).

4. Discussion

4.1. Ammonium migration and transformations: spatial variability

The inflow water employed in the systems showed NH_4^+ concentrations ranging from 0.93 to 5.54 mM, with $\delta^{15}N$–NH_4^+ ranging from +8.2‰ to + 10.4‰. These values are in agreement with an organic pollution source (Smith and Miller, 2006) as expected since the inflow water is urban wastewater and a wastewater discharge from nearby hospitals. NH_4^+ concentration in the inflow water showed an annual maximum in summer attaining a peak concentration in September (Fig. 6) which could be attributed to the population increase that doubles during summer months, linked to tourism, which implies a higher sewage input of organic N.

Microbial oxidation of NH_4^+ to NO_3^- (nitrification) appears to be the main transformation mechanism of the inorganic N (NH_4^+ + NO_3^-) species in the systems. During nitrification, NH_4^+ concentration decreases coupled with an O_2 decrease and an increase of NO_3^- concentration along the flow path. Considering nitrification as the only reaction that produces the decrease of NH_4^+ in the systems, an increase of NO_3^- is expected following the stoichiometry of the reaction (Eq. (1) and (1) mol of NO_3^-).

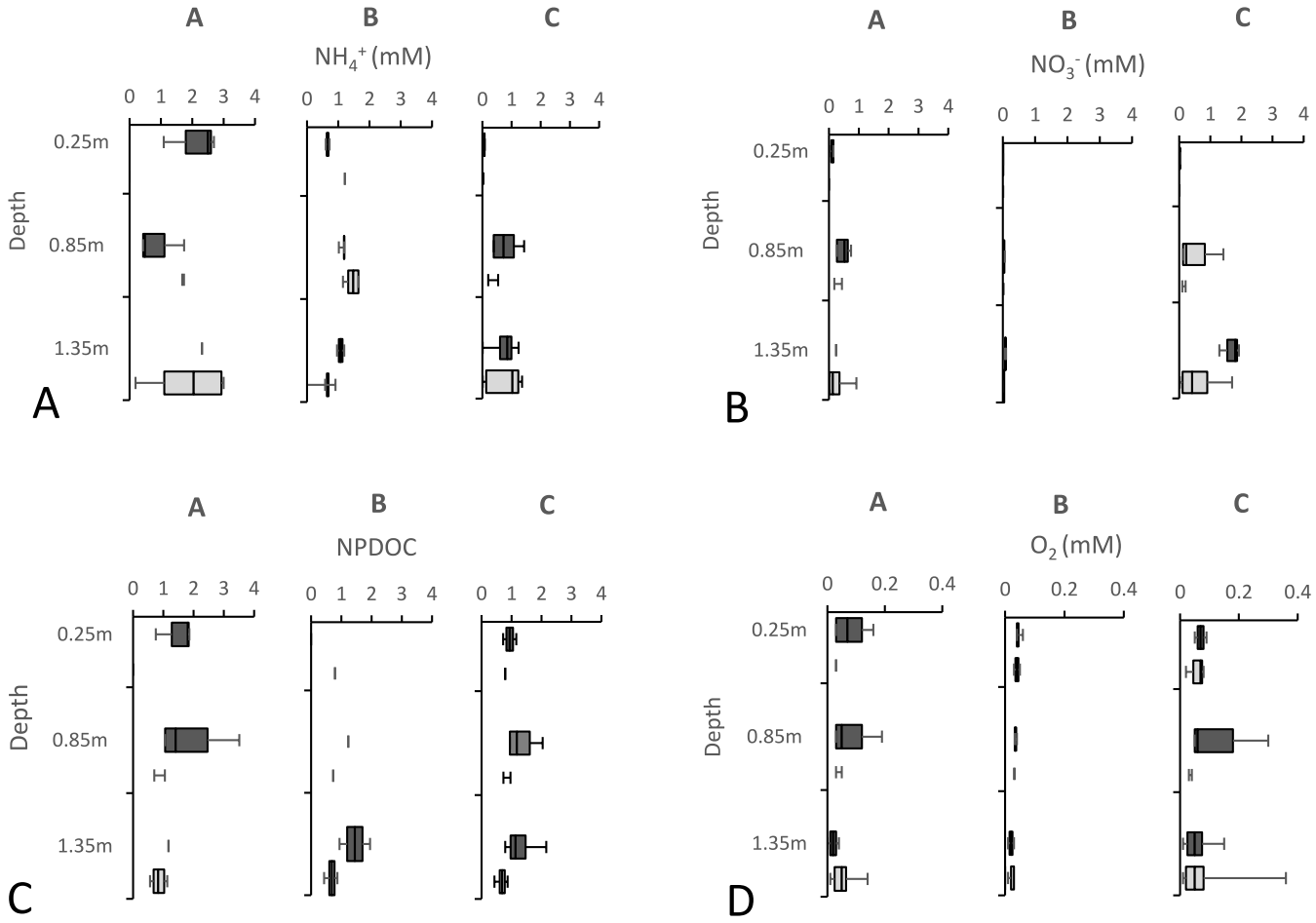

Fig. 4. The evolution of NH_4^+ (A figure), NO_3^- (B figure), NPDOC (C figure) and O_2 (D figure) aqueous concentration with depth at A, B and C sections in the systems (Concentrations are indicated by the box plots and the outliers represented by the dots plotted using all temporal series. First boxplot at each depth (light grey) = SAT-Control system and the second boxplot (dark grey) = SAT-PRB system.

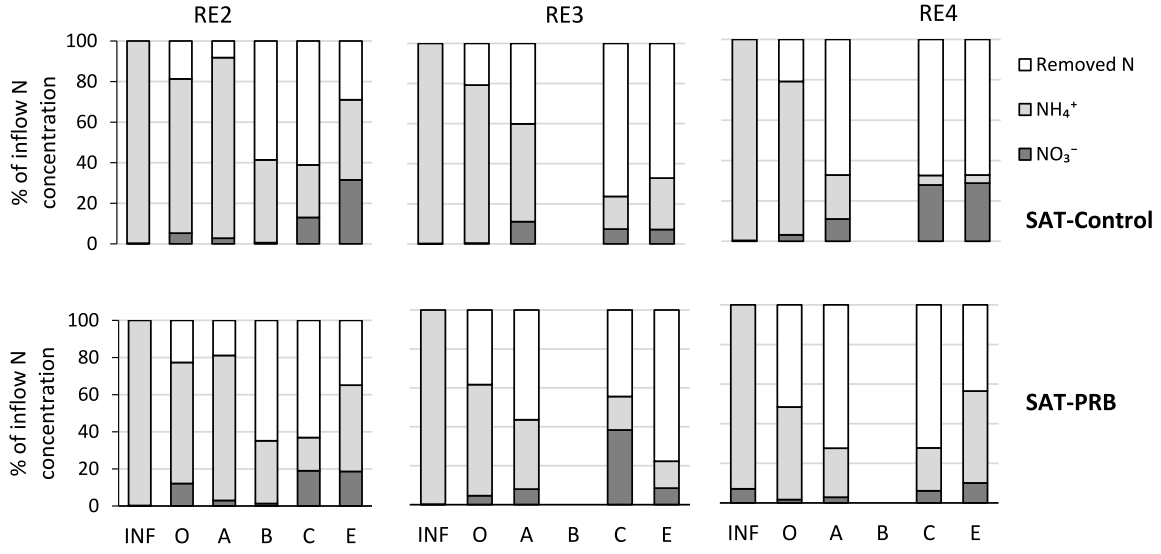

Fig. 5. Comparison of the % distribution of inflow NH_4^+, residual NO_3^-, and nitrogen removed along the flow path in the systems for all depth profiles during each recharge episode for SAT-Control (top) and SAT-PRB (bottom) systems.

However, the measured NO_3^- concentration in the field does not match this stoichiometry. Total N measured in water is below the expected value, suggesting that other processes may be responsible for N removal. The deficit in N ($N_{deficit}$) along the flow path in the systems (Fig. 5) can be calculated as the difference between the total N in the inflow water and the residual N dissolved in solution (Eq. 4).

$$N_{deficit} = N\text{-}NH_4^+ INF - \left(N\text{-}NH_4^+ res + N\text{-}NO_3^- res\right) \quad (4)$$

where $N\text{–}NH_{4INF}^+$ is the NH_4^+ concentration in the inflow water (nitrate was negligible in the inflow, Table S1), $N\text{–}NH_{4res}^+$ and $N\text{–}NO_{3res}^-$ are the residual concentration of NH_4^+ and NO_3^- in each sample point in the system. The observed N deficit can be explained either by NH_4^+ consumption or by another process such as sorption of NH_4^+ (Alshameri et al., 2018; Fidel et al., 2018; Wang et al., 2015) or plant assimilation (Desimone and Howes, 1998; Lusby et al., 1998) or due to contemporaneous production and consumption of nitrates (coupled nitrification-denitrification reaction) (Kim et al., 1997; Lusby et al., 1998; Smith et al., 2006) or Anammox reactions (Burgin and Hamilton, 2007; Castro-barros et al., 2017). In fact, genetic analyses of the microbial communities present in the barriers demonstrate a potential for all these microbially mediated processes to occur (Hellman et al., 2022). Clay is a component of the PRB and it could provide sorption sites for cation exchange. Since no isotopic fractionation is expected during sorption, comparing the $\varepsilon^{15}N\text{–}NH_4^+$ for the different recharge periods cannot confirm or discard its occurrence. Still, sorption will not affect dramatically long-term N removal processes because its main effect is to buffer inflow fluctuations, which is confirmed by the fact that similar $\varepsilon^{15}N\text{–}NH_4^+$ was observed in the SAT-PRB system in all recharge episodes (Table S1) and explained further in the section dealing with isotopic fractionation.

Plant assimilation could be relevant in the recharge area, especially during plant growth at the beginning of the study. Nevertheless, plant assimilation is reduced once plants are fully grown, and plant decay can also contribute as a source of organic N in the systems. Denitrification can also be important, especially after infiltration, when O_2 concentration is low. The latter hypothesis is confirmed using the $\delta^{15}N$ and $\delta^{18}O$ of NO_3^- since the highest values for these parameters were observed at O and A in both the SAT-Control and SAT-PRB systems. This suggests that part of the NO_3^- produced by nitrification is quickly reduced due to the low O_2 and high NPDOC. A plot of ^{15}N vs. ^{18}O confirms that denitrification is taking place in the systems (Fig. 7 C).

During the RE-2 and RE-3, NH_4^+ concentration removed along the SAT-PRB system was significantly higher than in the SAT-Control system (Fig. 3A). More efficient nitrification was expected in the SAT-Control system, than in the SAT-PRB system where O_2 is used to degrade its higher NPDOC, thus inhibiting nitrification as reported in previous groundwater and nitrifying biofilm studies (Jie et al., 2009; Ling and Chen, 2005). The unexpected higher removal rate of NH_4^+ may be linked to sorption but the higher $\delta^{15}N\text{–}NH_4^+$ values measured in the SAT-PRB system support that nitrification was higher in this system. We attribute this paradox to the NO_3^- produced from nitrification of NH_4^+ is then denitrified upon reaching the PRB due to reducing conditions created at the reactive barrier base (O) as the NPDOC consumes O_2 in the inflow water.

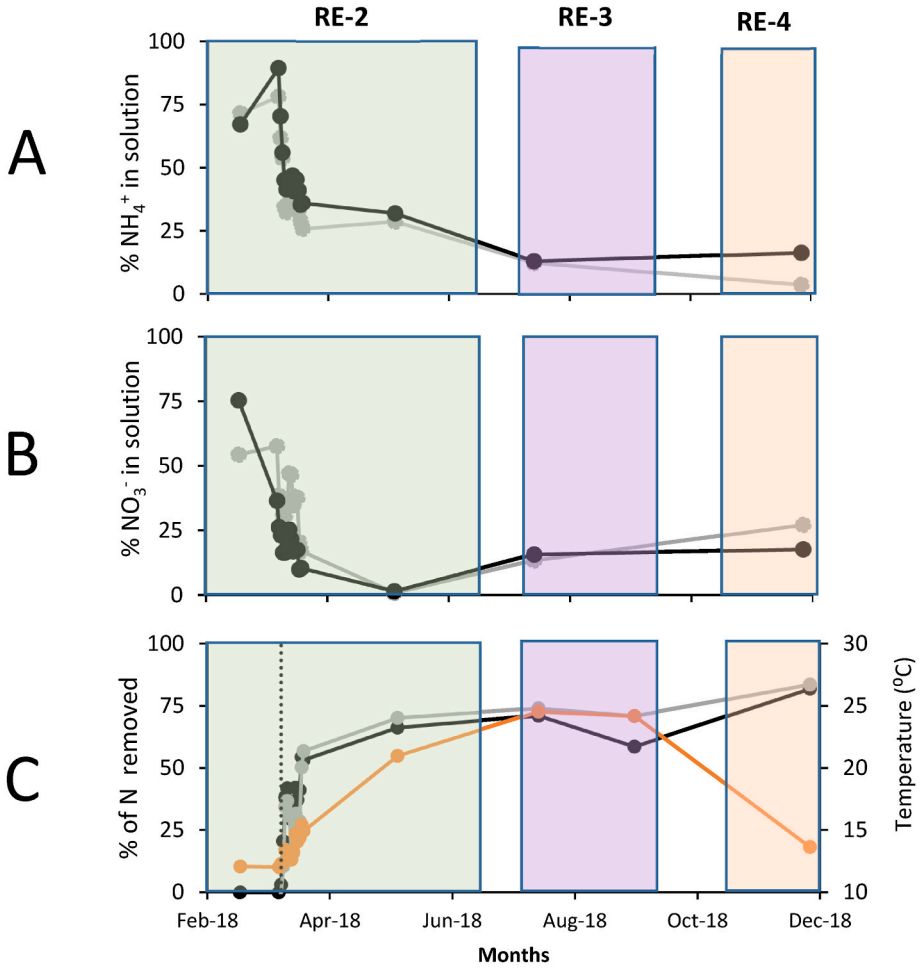

Fig. 6. (A) % distribution of residual NH_4^+ in solution at E; (B) % distribution of residual NO_3^- in solution at E; (C) the % of N (NH_4^+ + NO_3^-) removed from the solution and the average temperature in both systems. Grey circles represent the SAT-Control system, black circles represent the SAT-PRB system, and orange circles represent the average temperature in both systems. The dotted line represents the point below which we have zero N removal from the systems. (For interpretation of the references to colour in this figure legend, the reader is referred to the Web version of this article.)

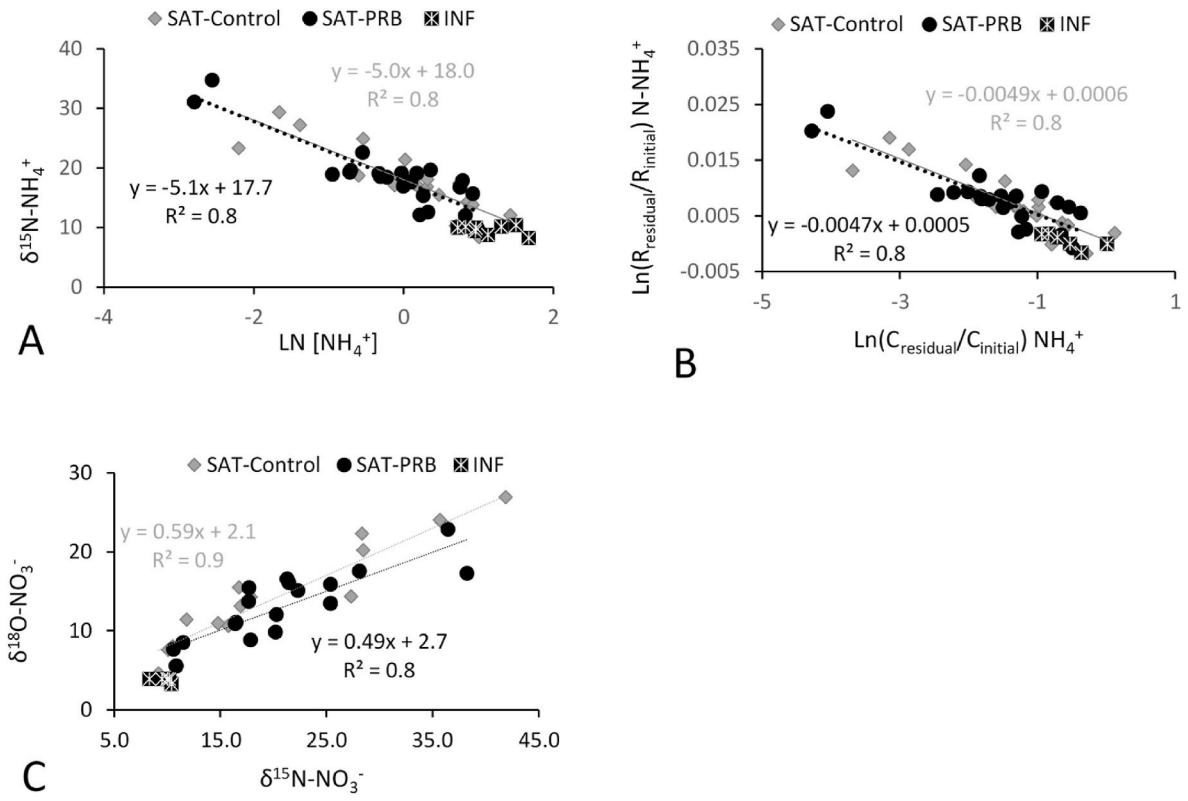

Fig. 7. Evolution of $\delta^{15}N–NH_4^+$ versus $[NH_4^+]$ in SAT-Control and SAT-PRB systems (A and B). Relationship between $\delta^{15}N–NO_3^-$ and $\delta^{18}O–NO_3^-$ during NO_3^- degradation in systems, (C).

4.2. Nitrate production and reduction: spatial variability

No significant change in NO_3^- concentration along the flow path from O to C was observed but a significant increase at the outlet was detected in both systems. The increase in NO_3^- at the outlets (E) could be explained by an increased nitrification rate favored by flux of O_2, which we attribute to the grama grass prevalent in the canals. The isotopic evolution of NO_3^- along the flow path showed typical denitrification trends suggesting that this reaction could be taking place. Both nitrification and organic carbon oxidation favour anoxic conditions in the systems; the observed NO_3^- reduction could, therefore, be linked to NPDOC consumption providing energy for denitrifying bacteria. Nonetheless, dissimilatory NO_3^- reduction to NH_4^+ (DNRA) might have contributed to NO_3^- removal as well. However, the $N_{deficit}$ (Eq. (4)) observed cannot be explained by DNRA suggesting that denitrification was the principal NO_3^- removal process.

At each particular section, maximum NH_4^+ accumulation was observed at the bottom of the systems (Fig. 4) suggesting that the rate of nitrification decreased with depth. More aerobic conditions prevailing in the shallower part of the systems favored nitrification resulting in higher nitrification occurring at the top of the systems which is consistent with studies on nitrification-denitrification rates reported in the literature (Kim et al., 1997; Smith et al., 2006). The upper points of our systems are in contact with the atmosphere so oxygen diffusion can account for these higher values at the top. Maximum NO_3^- was not observed at the top of our systems due to the contemporaneous production and consumption of NO_3^- The higher rate of nitrification at the top of the systems produced a higher consumption of O_2 creating anoxic conditions for denitrification to occur. This assumption is consistent with the high concentration of NH_4^+ and low O_2 observed at the bottom of the systems (Fig. 4).

In the SAT-Control system, NPDOC decreases with depth but the variability of SAT-PRB is due to the release of DOC from the barrier and the different travel times of the water at the bottom of the systems. The water flow in the bottom of the systems is slower than in the middle and the top of the systems where flow is faster (based on the tracer tests performed data not shown). Therefore, the water flowing through the bottom of the systems has more time for the DOC to degrade.

4.3. Temporal variability of NO_3^- and NH_4^+ production and reduction rates at the outlet

It was observed that the processes responsible for N attenuation in the systems were more effective during RE-3 (July to September) as NH_4^+ concentration decreased from 4.19 mM in the inflow to 0.69 mM at the C section in the SAT-Control system and 0.58 mM in the outlet of the SAT-PRB system (Fig. 3). Low residual NO_3^- concentration was measured suggesting a high denitrification rate during RE-3. For example, 31.5% (RE-2), 7.2% (RE-3) and 28.9% (RE-4) of the total N were measured in the SAT-Control system and 18.7% (RE-2), 8.5% (RE-3) and 10.8% (RE-4)) of the total N was measured in the SAT-PRB system at the outlet. Temperatures measured at the infiltration water increased from 12.0 °C to 24.2 °C (March to May) during RE-2, from 26.1 °C to 29.3 °C (July to September) during RE-3 and decreased to 15.4 °C from October to December during RE-4. High N attenuation during RE-3 could be attributed to the high temperature and the rapid acclimatization of the latent denitrifying bacteria at the beginning of RE-3 (Margalef-Marti et al., 2019). The dry periods between the recharge episodes did not significantly influence N attenuation in the systems. At the start of RE-2, RE-3 and RE-4, the latent biomass community might have quickly adapted when recharge resumed.

During 3 days in March 2018, residual N at the outlet (E) of the systems was higher than the total inorganic N ($NH_4^+ + NO_3^-$) in the inflow water (INF) (Fig. 6C). This reflects the sudden drop in inflow concentration due to a storm (a unitary sewage system feeds the WWTP so that wastewater is diluted during rain events). It is therefore assumed

zero N removal in the systems during this period (February 16, 2018 to March 27, 2021) as depicted in Fig. 6C.

Residual inorganic N progressively decreased in the outflow of the systems beyond the March event (dotted line in Fig. 6C). Biomass growth and adaptation in the systems coupled with the increasing temperatures during the warm period may have increased the N removal rates, thereby, decreasing the residual inorganic N along time. The average N removal rate increased from 31% of the total discharged N (RE-2) to 72% (RE-3) and from 38% (RE-2) to 65% (RE-3) in the SAT-Control and the SAT-PRB systems respectively (Fig. 6C). In both cases, the % increase of the N removal rate from RE-2 to RE-3 suggests that temperature played a significant role in the N removal from the systems (Fig. 6C). Still, while acknowledging the impact of temperature, the fact that N removal continued to increase during RE-4 when temperatures dropped, suggests that microbial community growth and adaptation also played a significant role. The NH_4^+ progressively decreased from 72% to 4% of total N inflow in the SAT-Control system and 67%–16% in the SAT-PRB system while NO_3^- decreased from 54% to 27% (0.80 mM) of total N inflow in the SAT-Control system and from 75% to 18% in the SAT-PRB system measured at the outlets at the end of the study period (Fig. 6B). The significant fluctuations observed may be attributed to the composition of the recharge water during the recharge episodes, fluctuations in the inflow concentrations (population seasonality and rainfall), and variations in biomass during non-recharge periods, which affect the prevailing reactions. The residual N measured at the outlet of both systems are very similar. However, differences were observed in the dominant N species measured at the outlet of the two systems and the recharge periods. For the SAT-Control system, during RE-2, NH_4^+ was the main N form (1% NO_3^- and 29% NH_4^+), during RE-3 an approximately equal proportion of NO_3^- and NH_4^+ was observed (14% NO_3^- and 13% NH_4^+) and finally, during RE-4 NO_3^- was the dominant species (27% NO_3^- and 4% NH_4^+) (Fig. 6A and B). For the SAT-PRB system, NH_4^+ was also the dominant species (2% NO_3^- and 32% NH_4^+) in RE-2, and during both RE-3 and RE-4 an approximately equal proportion of NO_3^- and NH_4^+ was observed (16–18% NO_3^- and 13–16% NH_4^+) (Fig. 6A and B).

4.4. Isotopic fractionation

NH_4^+ and NO_3- transformations are often characterized by isotopic fractionation (Casciotti et al., 2003; Mariotti et al., 1981), which reflects that reaction rates depend on the isotopes (Casciotti et al., 2011). The degree of fractionation is affected by the extent of substrate consumption, and processes that compete for the substrate (Wankel et al., 2007). The magnitude of fractionation is characterized using the Rayleigh distillation equation, which expresses a power law relationship between the evolution of the isotopic ratio ($R = \delta + 1$) and that of the species concentration, or more conveniently.

$$\mathrm{Ln}\left(\frac{R_{residual}}{R_{initial}}\right) = \varepsilon\ \mathrm{Ln}\left(\frac{C_{residual}}{C_{initial}}\right) \quad (5)$$

where ε is the isotope enrichment factor. This equation can be linearized as.

$\delta_{residual} = \varepsilon\ (1 + \delta_{initial})\mathrm{Ln}(C_{residual}/C_{initial})$. Indeed, a linear correlation was observed in both systems between $\delta^{15}N–NH_4^+$ and the natural logarithm (Ln) of the residual NH_4^+ (Fig. 7A). The resulting enrichment factor ($\varepsilon^{15}N–NH_4^+$) in the SAT-Control and the SAT-PRB systems was −5‰ ($R^2 = 0.8$). That is, the transformation of NH_4^+ to NO_3^- resulted in an increased $\delta^{15}N–NH_4^+$ in the residual NH_4^+ pool. The lighter isotopes ($\delta^{14}N–NH_4^+$) are preferentially incorporated into the generated NO_3^- resulting in $\delta^{15}N–NH_4^+$ enriched residual NH_4^+ and low $\delta^{15}N–NO_3^-$ in the generated NO_3^-. This is consistent with similar studies of NH_4^+ migration and reaction in contaminated groundwater where a decrease in NH_4^+ concentration yielded an increase in $\delta^{15}N–NH_4^+$ (Smith and Miller, 2006; Venkiteswaran et al., 2019). $\varepsilon\ ^{15}N–NH_4^+$ values reported in the literature for nitrification range from −10‰ to −28‰ in laboratory culture and field-scale studies (Sebilo et al., 2006). Lower $\varepsilon^{15}N–NH_4^+$ (in absolute values) could be explained by some potential contribution of plant assimilation in the systems. Hellman et al. (2022) suggested that the mixed vegetation at the infiltration area contributed to the NH_4^+ attenuation in the SAT-PRB system at the beginning of the experiment. The assimilation of $N–NH_4^+$ by different plant species reported by Emmerton et al. (2001), estimated an increase in $\delta^{15}N–NH_4^+$ of 2‰. The study on the uptake of ionic NH_4^+ by two plant species by Yoneyama et al. (2001) showed that the magnitude of the uptake of NH_4^+ depended on the concentrations of NH_4^+ and the plant species with $\varepsilon^{15}N–NH_4^+$ ranging from −2 to −8.1‰ and −3.9 and −24.1‰ for low concentrations of NH_4^+ (0.04–0.2 mM) and −9.4 to −18‰ and −13.4 to −28.9‰ at high concentrations (0.5–4 mM). Consequently, it is somewhat difficult to distinguish between nitrification and plant assimilation isotopically. In the systems, evaluated plant assimilation must be mainly located in the infiltration area and limited to the shallowest portions of the canals, where vegetation is limited and surficial. The vertical transport of atmospheric O_2 into the systems resulted in a high rate of nitrification between sections A, B and C. The diffused O_2 was consumed during nitrification keeping its content similar to the O_2 in the infiltrated water. Note, however, that the conditions (relatively high concentrations of both electron donors and acceptors) favour a highly dynamic biological activity, with relatively fast growth of biofilms and parallel changes in redox conditions (Carrera et al., 2022). Results of $\delta^{15}N–NH_4^+$ in our systems showed constant isotopic fractionation from O to the outlets (Fig. 6B). This can be explained by two hypotheses. The first is that assimilation and nitrification have similar fractionation. The second hypothesis is that fractionation related to assimilation is limited and the main process affecting the isotopic composition of $\delta^{15}N–NH_4^+$ would be nitrification.

The low $\delta^{15}N–NO_3^-$ in the generated nitrate compared to $\delta^{15}N–NH_4^+$ can be explained by the preferential incorporation of the lighter isotopes to the nitrate substrate produced by nitrification. The increase in $\delta^{15}N–NO_3^-$ and $\delta^{18}O–NO_3^-$ in the systems was associated with a corresponding decrease in the residual nitrate concentration linked to denitrification. This was evidenced as the NO_3^- concentration decreased from 1.24 mM to 0.8 mM in the SAT-Control system and from 1.72 mM to 0.52 mM in the SAT-PRB system measured at the outlets (end of the monitoring period). A linear correlation between $\delta^{15}N–NO_3^-$ and $\delta^{18}O–NO_3^-$ evolution in the systems is observed with slopes of 0.6 and 0.5 in the SAT-Control and the SAT-PRB systems, respectively (Fig. 7C). The deviation of $\delta^{15}N–NO_3^-$:$\delta^{18}O–NO_3^-$ from the 1:1 linear relationship can be explained by (I) the variance of the $\delta^{18}O$ of the O atom donors (O_2: H_2O = 1:2) during the oxidation of NH_4^+ to hydroxylamine NH_2OH to NO_2^- and NO_2^- to NO_3^- (Kumar et al., 1983) (II) O isotope exchange and fractionation (Martin and Casciotti, 2016).

Several authors have reported diverse $\varepsilon\ ^{15}N–NO_3^-$ and $\varepsilon\ ^{18}O–NO_3^-$ for groundwater studies ranging from −8.6‰ to −22.9‰ and −5.5‰ to −18.3‰ for $\varepsilon\ ^{15}N–NO_3^-$ and $\varepsilon\ ^{18}O–NO_3^-$ respectively (Carrey et al., 2013; Fukada et al., 2003). However, in the present experiment, the linear relationship typical for microbial nitrate reduction between $\delta^{15}N–NO_3^-$, $\delta^{18}O–NO_3^-$ and the natural logarithm of the residual NO_3^- was not observed (Fig. S3). As there is NO_3^- production and reduction at the same time $\varepsilon\ ^{15}N–NO_3^-$ and $\varepsilon\ ^{18}O–NO_3^-$ could not be modelled as a closed system using the Rayleigh model. This limits the use of isotopes to quantify NO_3^- degradation in coupled nitrification-denitrification systems. Fig. 8 shows $\delta^{15}N–NO_3^-$ and $\delta^{18}O–NO_3^-$ and the substrate remaining fraction from the present study using literature $\varepsilon\ ^{15}N–NO_3$ and $\varepsilon\ ^{18}O–NO_3$ produced by compost ($\varepsilon\ ^{15}N–NO_3^-$ = -10.4‰, $\varepsilon\ ^{18}O–NO_3^-$ = -9‰) (Grau-Martínez et al., 2017) and low $\varepsilon\ ^{15}N–NO_3$ and $\varepsilon\ ^{18}O–NO_3$ of −3‰. Some samples follow the trend expected for denitrification as NO_3^- fraction decreases. However, some samples of a very low fraction of residual NO_3^- showed lower $\delta^{15}N–NO_3^-$ and $\delta^{18}O–NO_3^-$ close to initial isotopic composition. This can be explained considering that in some areas of the systems, denitrification was able to completely remove NO_3^- and, after that, nitrification continues producing new NO_3^- that would have lower

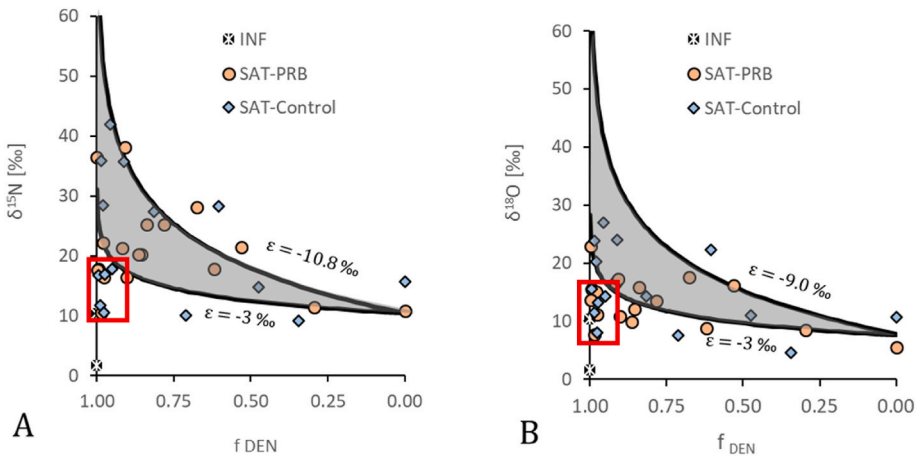

Fig. 8. Isotopic fractionation for $\varepsilon^{15}N–NO_3^-$ = −10.8‰ (solid line) and −3.0‰ (dashed line) (A) and $\varepsilon\ ^{18}O–NO_3^-$ = −9‰ (solid line) and 3.0‰ (dashed line) (B) using the Rayleigh equation. The shaded region shows the evolution of $\delta^{15}N–NO_3^-$ and $\delta^{18}O–NO_3^-$ between ε −10.8‰ and −3.0‰ (A) and −9‰ and −3.0‰ (B) normally observed in denitrification studies in similar conditions (Grau-Martínez et al., 2017). Dots and square boxes are $\delta^{15}N–NO_3^-$ and $\delta^{18}O–NO_3^-$ experimental data in MAR-PRB and SAT-Control systems. The asterisks show $\delta^{15}N–NO_3^-$ and $\delta^{18}O–NO_3^-$ in the inflow (INF) and the box highlights the $\delta^{15}N–NO_3^-$ and $\delta^{18}O–NO_3^-$ values that do not fall between the fractionation (extreme deviation).

$\delta^{15}N–NO_3^-$ and $\delta^{18}O–NO_3^-$. The linearity of $\delta^{15}N$ and $\delta^{18}O$ and the natural logarithm of the residual NO_3^- during reduction can, therefore, be affected by the mixing of newly generated NO_3^- with the residual NO_3^- in the substrate pool for nitrification-denitrification processes in the present study.

5. Conclusion

We studied the removal of dissolved N from N-contaminated inflow water in two SAT mesocosm systems. Conventional SAT and SAT-PRB systems were compared. Results showed that both systems are efficient in removing N since the net N removed reached up to 69% in the conventional SAT and 66% in the SAT-PRB, and this removal seems to grow with time and be temperature-dependent. Contemporaneous production and consumption of NO_3^- (nitrification-denitrification) were the principal processes active in the systems. The NH_4^+ and NO_3^- isotopic characterization confirmed that nitrification and denitrification were accompanied by the enrichment of the residual substrate concentration in heavy isotopes. The isotopic fractionation associated with NO_3^- degradation could not be obtained in this study due to constant production and reduction of NO_3^-.

The plant compost in the SAT-PRB system installed to favour CECs removal did not introduce a significant change in the global N removal. The isotopic fractionation calculated for $\delta^{15}N–NH_4^+$ was −5‰ in both systems. The residual inorganic N remained in the SAT-Control system predominantly as NO_3^- and in the SAT-PRB as equal proportions of NH_4^+ and NO_3^-, suggesting that the plant compost in the PRB increased the electron donor source and contributed to the higher rate of denitrification in the SAT-PRB system.

The concentration of NO_3^- in inflow water was below the EU nitrate threshold limit (50 mg/L - NO_3^-) throughout the whole experiment in the SAT-PRB system except at the beginning of the first recharge episode (average = 33.2 mg/L). In the SAT-Control system, the concentration of NO_3^- in the inflow water was above the EU nitrate threshold limit during the entire experiment except during the warm periods when the temperature was high (average = 51.4).

The concentration of NH_4^+ in the inflow water in both systems was above the maximum EU threshold value for NH_4^+ (5 mg/L - NH_4^+) throughout the entire experiment (average = 55.0 mg/L in the SAT-PRB system, and 54.5 mg/L in the SAT-Control system). The presence of PRB favored the removal of NO_3^- with time. The SAT-PRB had NO_3^- below safe water drinking limit, but NH_4^+ above safe water drinking limit and the SAT-Control system had both NO_3^- and NH_4^+ above safe water drinking limit, rendering water from both systems inappropriate for direct human consumption.

Funding

This work has been financed by the following projects: EU project ACWAPUR (Water JPI -WaterWorks 2014 code PCIN-2015-239), PACE-ISOTEC (CGL2017-87216-C4-1-R) financed by the Spanish Government and AEI/FEDER from the UE, the Water JPI (MARadentro-PCI2019-103603), the project RESTORA (CA210/18/00040) from the Catalan Water Agency, and the Consolidated Research Group MAG (2017-SGR-1733), financed by the Catalan Government. IDAEA-CSIC is a Center of Excellence Severo Ochoa (Spanish Ministry of Science and Innovation, Project CEX2018-000794-S).

The EU Water JPI project MARADENTRO (PCI2019-103603-WW2017), the Catalan Research Project RESTORA (ACA210/18/00040) and AGAUR (AQU - 2017 SGR 1485).

Authorship statement

All authors certify that they have participated sufficiently in the work to take public responsibility for the content, including participation in the concept, design, analysis, writing, or revision of the manuscript. Furthermore, each author certifies that this material or similar material has not been and will not be submitted to or published in any publication before its appearance in the *Journal of Environmental Management*.

Conception and design of study: C. Valhondo, L. Martínez-Landa, R. Carrey, J. Carrer, N.Otero; acquisition of data: R. Carrey, C. Valhondo, L. Martínez-Landa; analysis and/or interpretation of data: A. Abu, R. Carrey, C. Valhondo, L. Martínez-Landa; Drafting the manuscript: A. Abu, R. Carrey; revising the manuscript critically for important intellectual content: C. Valhondo, C. Domènech, A. Soler, S. Diaz-Cruz, L. Martínez-Landa, R. Carrey, J. Carrera, N. Otero; Approval of the version of the manuscript to be published (the names of all authors must be listed): C. Domènech, A. Soler, S. Diaz-Cruz, A. Abu, L. Martínez-Landa, C. Valhondo, R. Carrey, J. Carrera, N. Otero.

Declaration of competing interest

The authors declare that they have no known competing financial interests or personal relationships that could have appeared to influence the work reported in this paper.

Data availability

Data will be made available on request.

Acknowledgements

The authors are grateful to Consorci de la Costa Brava Girona (CCBGi), the staff of the Palamós WWTP for their unconditional help, and the AGAUR-SGR2017-1485 research group. Abu Alex would like to thank the The Agency for Management of University and Research Grants of the Generalitat de Catalunya for the Ph.D. grant (2019 FI_B 01059) and the CCiT of University of Barcelona for the analytical support.

Appendix A. Supplementary data

Supplementary data to this article can be found online at https://doi.org/10.1016/j.jenvman.2022.115927.

References

Adebowale, T., Surapaneni, A., Faulkner, D., McCance, W., Wang, S., Currell, M., 2019. Science of the Total Environment Delineation of contaminant sources and denitrification using isotopes of nitrate near a wastewater treatment plant in peri-urban settings. Sci. Total Environ. 651, 2701–2711. https://doi.org/10.1016/j.scitotenv.2018.10.146.

Alshameri, A., He, H., Zhu, J., Xi, Y., Zhu, R., Ma, L., Tao, Q., 2018. Applied Clay Science Adsorption of ammonium by different natural clay minerals : Characterization. kinetics and adsorption isotherms 159, 83–93. https://doi.org/10.1016/j.clay.2017.11.007.

Arauzo, M., 2017. Vulnerability of groundwater resources to nitrate pollution: a simple and effective procedure for delimiting Nitrate Vulnerable Zones. Sci. Total Environ. 575, 799–812. https://doi.org/10.1016/j.scitotenv.2016.09.139.

Baú, D.A., Mayer, A.S., 2008. Optimal design of pump-and-treat systems under uncertain hydraulic conductivity and plume distribution. J. Contam. Hydrol. 100, 30–46. https://doi.org/10.1016/j.jconhyd.2008.05.002.

Beauchamp, E.G., Trevors, J.T., Paul, J.W., 1989. Carbon Sources for Bacterial Denitrification 10, 113–142. https://doi.org/10.1007/978-1-4613-8847-0_3.

Bourke, S.A., Iwanyshyn, M., Kohn, J., Jim Hendry, M., 2019. Sources and fate of nitrate in groundwater at agricultural operations overlying glacial sediments. Hydrol. Earth Syst. Sci. 23, 1355–1373. https://doi.org/10.5194/hess-23-1355-2019.

Burgin, A.J., Hamilton, S.K., 2007. Have we overemphasized the role of denitrification in aquatic ecosystems? A review of nitrate removal pathways. Front. Ecol. Environ. 5, 89–96. https://doi.org/10.1890/1540-9295, 2007)5[89:HWOTRO]2.0.CO;2.

Carrera, J., Saaltink, M.W., Soler-Sagarra, J., Wang, J., Valhondo, C., 2022. Reactive transport: a review of basic concepts with emphasis on biochemical processes. Energies 15 (3), 925. https://doi.org/10.3390/en15030925.

Carrey, R., Otero, N., Soler, A., Gómez-Alday, J.J., Ayora, C., 2013. The role of Lower Cretaceous sediments in groundwater nitrate attenuation in central Spain: column experiments. Appl. Geochem. 32, 142–152. https://doi.org/10.1016/j.apgeochem.2012.10.009.

Casciotti, K.L., Sigman, D.M., Ward, B.B., 2003. Linking diversity and stable isotope fractionation in ammonia-oxidizing bacteria. Geomicrobiol. J. 20, 335–353. https://doi.org/10.1080/01490450303895.

Casciotti, K.L., Buchwald, C., Santoro, A.E., Frame, C., 2011. Assessment of nitrogen and oxygen isotopic fractionation during nitrification and its expression in the marine environment. In: Methods in Enzymology, first ed. Elsevier Inc. https://doi.org/10.1016/B978-0-12-381294-0.00011-0.

Castellano-Hinojosa, A., Charteris, A.F., Müller, C., Jansen-Willems, A., González-López, J., Bedmar, E.J., Carrillo, P., Cárdenas, L.M., 2020. Occurrence and 15N-quantification of simultaneous nitrification and denitrification in N-fertilised soils incubated under oxygen-limiting conditions. Soil Biol. Biochem. 143 https://doi.org/10.1016/j.soilbio.2020.107757.

Castro-barros, C.M., Jia, M., Loosdrecht, M.C.M., Van, Volcke, E.I.P., Winkler, M.K.H., 2017. Bioresource Technology Evaluating the potential for dissimilatory nitrate reduction by anammox bacteria for municipal wastewater treatment. Bioresour. Technol. 233, 363–372. https://doi.org/10.1016/j.biortech.2017.02.063.

Critchley, K., Rudolph, D.L., Devlin, J.F., Schillig, P.C., 2014. Stimulating in situ denitrification in an aerobic, highly permeable municipal drinking water aquifer. J. Contam. Hydrol. 171, 66–80. https://doi.org/10.1016/j.jconhyd.2014.10.008.

Desimone, L.A., Howes, L., 1998. Nitrogen transport and transformations in a shallow aquifer receiving wastewater discharge: a mass balance approach. Water Resour. Res. 34 (2), 271–285. https://doi.org/10.1029/97WR03040.

Díaz-Cruz, M.S., Barceló, D., 2008. Trace organic chemicals contamination in ground water recharge. Chemosphere 72, 333–342. https://doi.org/10.1016/j.chemosphere.2008.02.031.

Drewes, J.E., 2009. Ground water replenishment with recycled water - water quality improvements during managed aquifer recharge. Ground Water 47, 502–505. https://doi.org/10.1111/j.1745-6584.2009.00587_5.x.

Emmerton, K.S., Callaghan, T.V., Jones, H.E., Leake, J.R., Michelsen, A., Read, D.J., 2001. Assimilation and isotopic fractionation of nitrogen by mycorrhizal and nonmycorrhizal subarctic plants. New Phytol. 151, 513–524. https://doi.org/10.1046/j.1469-8137.2001.00179.x.

Fidel, R.B., Laird, D.A., Spokas, K.A., 2018. Sorption of ammonium and nitrate to biochars is electrostatic and pH-dependent. Sci. Rep. 1–10. https://doi.org/10.1038/s41598-018-35534-w.

Fukada, T., Hiscock, K.M., Dennis, P.F., Grischek, T., 2003. A dual isotope approach to identify denitrification in groundwater at a river-bank infiltration site, 37, pp. 3070–3078. https://doi.org/10.1016/S0043-1354(03)00176-3.

Gibert, O., Assal, A., Devlin, H., Elliot, T., Kalin, R.M., 2019. Performance of a field-scale biological permeable reactive barrier for in-situ remediation of nitrate-contaminated groundwater. Sci. Total Environ. 659, 211–220. https://doi.org/10.1016/j.scitotenv.2018.12.340.

Grau-Martínez, A., Torrentó, C., Carrey, R., Rodríguez-Escales, P., Domènech, C., Ghiglieri, G., Soler, A., Otero, N., 2017. Feasibility of two low-cost organic substrates for inducing denitrification in artificial recharge ponds: batch and flow-through experiments. J. Contam. Hydrol. 198, 48–58. https://doi.org/10.1016/j.jconhyd.2017.01.001.

Grau-Martínez, A., Folch, A., Torrentó, C., Valhondo, C., Barba, C., Domènech, C., Soler, A., Otero, N., 2018. Monitoring induced denitrification during managed aquifer recharge in an infiltration pond. J. Hydrol. 561, 123–135. https://doi.org/10.1016/j.jhydrol.2018.03.044.

Hellman, M., Valhondo, C., Martínez-Landa, L., Carrera, J., Juhanson, J., Hallin, S., 2022. Nitrogen removal capacity in microbial communities developing in compost- and woodchip-based multipurpose reactive barriers for aquifer recharge with wastewater. Front. Microbiol. 13 https://doi.org/10.3389/fmicb.2022.877990.

Jie, H.U., Daping, L.I., Qiang, L.I.U., Yong, T.A.O., Xiaohong, H.E., Xiaomei, W., Xudong, L.I., Ping, G.A.O., 2009. Effect of organic carbon on nitrification efficiency and community composition of nitrifying biofilms, 21, pp. 387–394. https://doi.org/10.1016/S1001-0742(08)62281-0.

Jokela, P., Eskola, T., Heinonen, T., Tanttu, U., Tyrväinen, J., Artimo, A., 2017. Raw water quality and pretreatment in managed aquifer recharge for drinking water production in Finland. Water (Switzerland) 9. https://doi.org/10.3390/w9020138.

Kim, D.H., Matsuda, O., Yamamoto, T., 1997. Nitrification, denitrification and nitrate reduction rates in the sediment of Hiroshima Bay, Japan. J. Oceanogr. 53, 317–324. https://doi.org/10.1016/S0967-0653(98)80283-4.

King, a., Jensen, V., Fogg, G.E., Harter, T., 2012. Groundwater remediation and management for nitrate. Addressing nitrate California's drink. Water with a focus tulare lake basin salinas val. Groundw 51.

Korom, S.F., 1992. Natural denitrification in the saturated zone: a review. Water Resour. Res. 28 (6), 1657–1668. https://doi.org/10.1029/92WR00252.

Kumar, S., Nicholas, D.J.D., Williams, E.H., 1983. Definitive 15N NMR evidence that water serves as a source of "O" during nitrite oxidation by Nitrobacter agilis. FEBS Lett. 152, 71–74. https://doi.org/10.1016/0014-5793(83)80484-0.

Kuster, M., Díaz-Cruz, S., Rosell, M., López de Alda, M., Barceló, D., 2010. Fate of selected pesticides, estrogens, progestogens and volatile organic compounds during artificial aquifer recharge using surface waters. Chemosphere 79, 880–886. https://doi.org/10.1016/j.chemosphere.2010.02.026.

Ling, J., Chen, S., 2005. Impact of organic carbon on nitrification performance of different biofilters. Aquacult. Eng. 33 (2), 150–162. https://doi.org/10.1016/j.aquaeng.2004.12.002.

Lusby, F.E., Gibbs, M.M., Cooper, A.B., Thompson, K., 1998. The fate of groundwater ammonium in a lake edge wetland. American Society of Agronomy, Crop Science Society of America, and Soil Science Society of America 27 (No. 2), 459–466. https://doi.org/10.2134/jeq1998.00472425002700020029x.

Maeng, S.K., Ameda, E., Sharma, S.K., Grützmacher, G., Amy, G.L., 2010. Organic micropollutant removal from wastewater effluent-impacted drinking water sources during bank filtration and artificial recharge. Water Res. 44, 4003–4014. https://doi.org/10.1016/j.watres.2010.03.035.

Margalef-Marti, R., Carrey, R., Soler, A., Otero, N., 2019. Evaluating the potential use of a dairy industry residue to induce denitrification in polluted water bodies: a flow-through experiment. J. Environ. Manag. 245, 86–94. https://doi.org/10.1016/j.jenvman.2019.03.086.

Mariotti, A., Germon, J.C., Hubert, P., Kaiser, P., Letolle, R., Tardieux, A., Tardieux, P., 1981. Experimental determination of nitrogen kinetic isotope fractionation: some principles; illustration for the denitrification and nitrification processes. Plant Soil 62, 413–430. https://doi.org/10.1007/BF02374138.

Martin, T.S., Casciotti, K.L., 2016. Nitrogen and oxygen isotopic fractionation during microbial nitrite reduction. Limnol. Oceanogr. 61, 1134–1143. https://doi.org/10.1002/lno.10278.

Matchett, L.S., Goulding, K.W.T., Webster, C.P., Haycock, N.E., 2019. Denitrification in Riparian Bu Er Zones: the Role of Floodplain Hydrology, vol. 13, pp. 10–11. https://doi.org/10.1002/(SICI)1099-1085(199907)13:10%3C1451::AID-HYP822%3E3.0.CO;2.

McIlvin, M.R., Altabet, M.A., 2005. Chemical conversion of nitrate and nitrite to nitrous oxide for nitrogen and oxygen isotopic analysis in freshwater and seawater. Anal. Chem. 77, 5589–5595. https://doi.org/10.1021/ac050528s.

Naidoo, S., Olaniran, A.O., 2013. Treated wastewater effluent as a source of microbial pollution of surface water resources. Int. J. Environ. Res. Publ. Health 11, 249–270. https://doi.org/10.3390/ijerph110100249.

Pabich, W.J., Valiela, I., Hemond, H.F., 2001. Relationship between DOC concentration and vadose zone thickness and depth below water table in groundwater of Cape Cod. U.S.A. Biogeochemistry 55, 247–268. https://doi.org/10.1023/A:1011842918260.

Ren, Y., Xu, Z., Zhang, X., Wang, X., Sun, X., Ballantine, D.J., Wang, S., 2014. Nitrogen pollution and source identification of urban ecosystem surface water in Beijing. Front. Environ. Sci. Eng. 8, 106–116. https://doi.org/10.1007/s11783-012-0474-z.

Robertson, W.D., Vogan, J.L., Lombardo, P.S., 2008. Nitrate removal rates in a 15-year-old permeable reactive barrier treating septic system nitrate. Ground Water Monit. Remed. 28, 65–72. https://doi.org/10.1111/j.1745-6592.2008.00205.x.

Ryabenko, E., Altabet, M.A., Wallace, D.W.R., 2009. Effect of chloride on the chemical conversion of nitrate to nitrous oxide for δ 15 N analysis. Limnol Oceanogr. Methods 7, 545–552. https://doi.org/10.4319/lom.2009.7.545.

Sebilo, M., Billen, G., Mayer, B., Billiou, D., Grably, M., Garnier, J., Mariotti, A., 2006. Assessing nitrification and denitrification in the Seine river and estuary using chemical and isotopic techniques. Ecosystems 9, 564–577. https://doi.org/10.1007/s10021-006-0151-9.

Shi, P., Zhang, Y., Song, J., Li, P., Wang, Y., Zhang, Xiaoming, Li, Z., Bi, Z., Zhang, Xin, Qin, Y., Zhu, T., 2019. Response of nitrogen pollution in surface water to land use and social-economic factors in the Weihe River watershed, northwest China. Sustain. Cities Soc. 50, 101658 https://doi.org/10.1016/j.scs.2019.101658.

Singleton, M.J., Esser, B.K., Moran, J.E., Hudson, G.B., Mcnab, W.W., Harter, T., 2007. Saturated zone denitrification: potential for natural attenuation of nitrate contamination in shallow groundwater under dairy operations. Environ. Sci. Technol. 41, 759–765. https://doi.org/10.1021/es061253g.

Smith, R.L., Miller, D.N., 2006. Ammonium Transport and Reaction in Contaminated Groundwater : Application of Isotope Tracers and Isotope Fractionation Studies, vol. 42, pp. 1–19. https://doi.org/10.1029/2005WR004349.

Smith, R.L., Baumgartner, L.K., Miller, D.N., Repert, D.A., Böhlke, J.K., 2006. Assessment of nitrification potential in ground water using short-term, single-well injection experiments. Microb. Ecol. 51, 22–35. https://doi.org/10.1007/s00248-004-0159-7.

Sonune, A., Ghate, R., 2004. Developments in wastewater treatment methods. Desalination 167, 55–63. https://doi.org/10.1016/j.desal.2004.06.113.

Union, European, 1991. Council directive of 12 december 1991 concerning the protection of waters against pollution caused by nitrates from agricultural sources. Directive 91/676/EEC. Off. J. Eur. Union L 375, 1–13.

Union, European, 2006. Directive 2006/118/EC of the European Parliament and of the Council of 12 December 2006 on the protection of groundwater against pollution and deterioration. Off. J. Eur. Union L 372, 19–31.

Valhondo, C., Carrera, J., Ayora, C., Barbieri, M., Nödler, K., Licha, T., Huerta, M., 2014. Behavior of nine selected emerging trace organic contaminants in an artificial recharge system supplemented with a reactive barrier. Environ. Sci. Pollut. Res. 21, 11832–11843. https://doi.org/10.1007/s11356-014-2834-7.

Valhondo, C., Carrera, J., Ayora, C., Tubau, I., Martinez-Landa, L., Nödler, K., Licha, T., 2015. Characterizing redox conditions and monitoring attenuation of selected pharmaceuticals during artificial recharge through a reactive layer. Sci. Total Environ. 512 (513), 240–250. https://doi.org/10.1016/j.scitotenv.2015.01.030.

Valhondo, C., Carrera, J., Martínez-Landa, L., Wang, J., Amalfitano, S., Levantesi, C., Diaz-Cruz, M.S., 2020a. Reactive barriers for renaturalization of reclaimed water during soil aquifer treatment. Water 12 (4), 1012. https://doi.org/10.3390/w12041012.

Valhondo, C., Martinez-Landa, L., Carrera, J., Díaz-Cruz, S.M., Amalfitano, S., Levantesi, C., 2020b. Six artificial recharge pilot replicates to gain insight into water quality enhancement processes. Chemosphere 240. https://doi.org/10.1016/j.chemosphere.2019.124826.

Venkiteswaran, J.J., Schiff, S.L., Ingalls, B.P., 2019. Quantifying the fate of wastewater nitrogen discharged to a Canadian river. Facets 4, 315–335. https://doi.org/10.1139/facets-2018-0028.

Volkmer, B.G., Ernst, B., Simon, J., Kuefer, R., Bartsch, G., Bach, D., Gschwend, J.E., 2005. Influence of nitrate levels in drinking water on urological malignancies: a community-based cohort study. BJU Int. 95, 972–976. https://doi.org/10.1111/j.1464-410X.2005.05450.x.

Wang, B., Lehmann, J., Hanley, K., Hestrin, R., Enders, A., 2015. Chemosphere Adsorption and desorption of ammonium by maple wood biochar as a function of oxidation and pH. Chemosphere 138, 120–126. https://doi.org/10.1016/j.chemosphere.2015.05.062.

Wankel, S.D., Kendall, C., Pennington, J.T., Chavez, F.P., Paytan, A., 2007. Nitrification in the euphotic zone as evidenced by nitrate dual isotopic composition: observations from Monterey Bay, California. Global Biogeochem. Cycles 21, 1–13. https://doi.org/10.1029/2006GB002723.

WHO, 2004. Guidelines for Drinking-Water Quality, third ed., vol. 1. WHO Libr. Cat. 1 https://apps.who.int/iris/handle/10665/42852.

Withers, P.J., Neal, C., Jarvie, H.P., Doody, D.G., 2014. Agriculture and eutrophication: where do we go from here? Sustainability 6 (9), 5853–5875. https://doi.org/10.3390/su6095853.

Yoneyama, T., Matsumaru, T., Usui, K., Engelaar, W.M.H.G., 2001. Discrimination of nitrogen isotopes, during absorption of ammonium and nitrate at different nitrogen concentrations by rice (Oryza sativa L.) plants. Plant Cell Environ. 24, 133–139. https://doi.org/10.1046/j.1365-3040.2001.00663.x.

Zhang, L., Altabet, M.A., Wu, T., Hadas, O., 2007. Sensitive measurement of NH4+15N/14N (δ15NH4+) at natural abundance levels in fresh and saltwaters. Anal. Chem. 79, 5297–5303. https://doi.org/10.1021/ac070106d.

Zirkle, K.W., Nolan, B.T., Jones, R.R., Weyer, P.J., Ward, M.H., Wheeler, D.C., 2016. Assessing the relationship between groundwater nitrate and animal feeding operations in Iowa (USA). Sci. Total Environ. 566–567, 1062–1068. https://doi.org/10.1016/j.scitotenv.2016.05.130.